Mycobacterium tuberculosis Lsr2 Is a Global Transcriptional Regulator Required for Adaptation to Changing Oxygen Levels and Virulence

I. L. Bartek,[a] L. K. Woolhiser,[b] A. D. Baughn,[c,d] R. J. Basaraba,[b] W. R. Jacobs, Jr.,[c] A. J. Lenaerts,[b] M. I. Voskuil[a]

Department of Microbiology, University of Colorado Denver, School of Medicine, Aurora, Colorado, USA[a]; Department of Microbiology, Immunology and Pathology, Colorado State University, Fort Collins, Colorado, USA[b]; Department of Microbiology and Immunology, Howard Hughes Medical Institute, Albert Einstein College of Medicine, Bronx, New York, USA[c]; Department of Microbiology, University of Minnesota, Minneapolis, Minnesota, USA[d]

ABSTRACT To survive a dynamic host environment, *Mycobacterium tuberculosis* must endure a series of challenges, from reactive oxygen and nitrogen stress to drastic shifts in oxygen availability. The mycobacterial Lsr2 protein has been implicated in reactive oxygen defense via direct protection of DNA. To examine the role of Lsr2 in pathogenesis and physiology of *M. tuberculosis*, we generated a strain deleted for *lsr2*. Analysis of the *M. tuberculosis* Δ*lsr2* strain demonstrated that Lsr2 is not required for DNA protection, as this strain was equally susceptible as the wild type to DNA-damaging agents. The *lsr2* mutant did display severe growth defects under normoxic and hyperoxic conditions, but it was not required for growth under low-oxygen conditions. However, it was also required for adaptation to anaerobiosis. The defect in anaerobic adaptation led to a marked decrease in viability during anaerobiosis, as well as a lag in recovery from it. Gene expression profiling of the Δ*lsr2* mutant under aerobic and anaerobic conditions in conjunction with published DNA binding-site data indicates that Lsr2 is a global transcriptional regulator controlling adaptation to changing oxygen levels. The Δ*lsr2* strain was capable of establishing an early infection in the BALB/c mouse model; however, it was severely defective in persisting in the lungs and caused no discernible lung pathology. These findings demonstrate *M. tuberculosis* Lsr2 is a global transcriptional regulator required for control of genes involved in adaptation to extremes in oxygen availability and is required for persistent infection.

IMPORTANCE *M. tuberculosis* causes nearly two million deaths per year and infects nearly one-third of the world population. The success of this aerobic pathogen is due in part to its ability to successfully adapt to constantly changing oxygen availability throughout the infectious cycle, from the high oxygen tension during aerosol transmission to anaerobiosis within necrotic lesions. An understanding of how *M. tuberculosis* copes with these changes in oxygen tension is critical for its eventual eradication. Using a mutation in *lsr2*, we demonstrate that the Lsr2 protein present in all mycobacteria is a global transcriptional regulator in control of genes required for adaptation to changes in oxygen levels. *M. tuberculosis* lacking *lsr2* was unable to adapt to both high and very low levels of oxygen and was defective in long-term anaerobic survival. Lsr2 was also required for disease pathology and for chronic infection in a mouse model of TB.

Address correspondence to Martin I. Voskuil, martin.voskuil@ucdenver.edu.

Mycobacterium tuberculosis is one of the most successful human pathogens, killing nearly two million people per year, and is the agent of an estimated two billion latent infections worldwide (1). The ability of *M. tuberculosis* to survive and to establish both active and latent infections despite the fact that the host is immunocompetent implies that the bacteria are able to survive insults from the host immune system, such as reactive oxygen species (ROS) and reactive nitrogen species (RNS). *M. tuberculosis* must also survive vast changes in oxygen tension, from high atmospheric oxygen levels during aerosol transmission to the microaerobic or anoxic environments within necrotic granulomas (2). The mechanisms employed by *M. tuberculosis* to protect itself from these stresses and changing environments during infection are not well understood. Deciphering the mechanisms that *M. tuberculosis* utilizes to survive these diverse conditions could

lead to more effective antibiotics and greater success in tuberculosis (TB) treatment.

The Lsr2 protein in mycobacterial species is similar to H-NS from *Escherichia coli* (3–6). H-NS works mainly to repress gene transcription by binding to AT-rich sequences in a sequence-independent fashion and has been implicated in virulence in *Shigella flexneri* and *Vibrio cholerae* (7). H-NS is able to activate gene expression as well, but examples of activation are less common (8). Lsr2 from *M. tuberculosis* and from *Mycobacterium smegmatis* has been shown *in vitro* to bind directly to DNA and protect it against H_2O_2 (9) and DNase I degradation (6). An *M. smegmatis lsr2* deletion mutant was also transiently more susceptible to H_2O_2 stress (9).

To examine the role of Lsr2 in *M. tuberculosis*, we deleted *lsr2* from the *M. tuberculosis* H37Rv strain. While *lsr2* has been re-
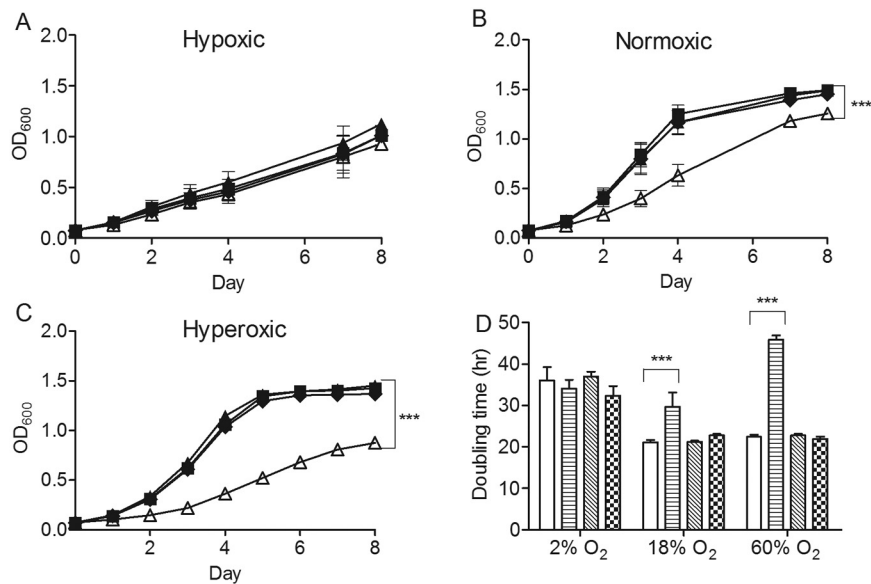
FIG 1 Growth of the Δlsr2 strain under hypoxic, normoxic, and hyperoxic oxygen tension. Cultures of H37Rv (squares and white bars), the Δlsr2 strain (open triangles and horizontally striped bars), the Δlsr2 complemented strain (diamonds and diagonally striped bars), or the lsr2 overexpression strain (closed triangles and checkered bars) were grown in DTA medium in either a chamber containing 2% oxygen (A), under atmospheric oxygen (~18% oxygen) (B), or a chamber containing 60% oxygen (C). (D) The doubling time was calculated from between day 1 and day 3 for each strain.

ported to be essential in *M. tuberculosis* (6, 10), we were able to generate a deletion mutation in *lsr2*. In contrast to the findings in *M. smegmatis*, we found the *M. tuberculosis* Lsr2 protein is not important for protection against DNA damage. The Lsr2 protein is, however, a global transcriptional regulator important for allowing *M. tuberculosis* to respond to changes in oxygen levels that would be experienced during both transmission and infection.

RESULTS

The Δ*lsr2* strain is sensitive to high-oxygen conditions. Initial experiments with the Δ*lsr2* strain demonstrated it was severely defective in initiating growth on solid agar plates. The lowest dilution formed a lawn, but all higher dilutions displayed highly defective growth (see Fig. S2 in the supplemental material). Cultures of the Δ*lsr2* strain, which had similar optical density at 600 nm (OD_{600}) and growth rate to the wild type under low-aeration conditions, displayed several logs less viability on Dubos-Tween-albumin (DTA) or 7H11 agar plates. These cultures displayed equal viability to the wild type when assayed using liquid culture to determine a most probable number (MPN). The liquid culture method was therefore used for all subsequent viability assessment. The Δ*lsr2* strain was defective for pellicle formation (see Fig. S3 in the supplemental material), as was previously shown in an *M. smegmatis* Δ*lsr2* mutant (3). We hypothesized these findings were due to the sensitivity of the mutant to the high-oxygen environment experienced by bacteria on the surface of an agar plate or at the surface of a bacterial liquid culture. Oxygen levels in air are 50 times higher than in liquid, even without factoring in the consumption of oxygen by bacteria in liquid culture. We therefore analyzed the growth of the four strains under hypoxic and hyperoxic conditions compared to growth under ambient air. Cultures were started at an OD_{600} of 0.1 and stirred either in an incubator containing ambient atmospheric oxygen or in an oxygen-controlled chamber containing a constant supply of oxygen at

either 2% or 60%. The Δ*lsr2* strain grew at the same rate as the wild-type strain under 2% oxygen (Fig. 1A). However, under atmospheric oxygen, the mutant showed a growth defect compared to the wild type (Fig. 1B). This growth defect was even more pronounced when the cultures were grown in 60% oxygen (Fig. 1C). As expected, the doubling time of all strains was greatest when grown in 2% oxygen compared to an 18% oxygen environment. However, whereas the growth rate of the wild type, the Δ*lsr2* complemented strain, and the *lsr2* overexpression strain did not change from 18% to 60% oxygen tension, the doubling time of the Δ*lsr2* strain increased significantly (Fig. 1D).

The Δ*lsr2* strain is not more sensitive to H_2O_2 or mitomycin C. In order to determine if the *M. tuberculosis* Δ*lsr2* strain was more sensitive to DNA-damaging agents, we exposed all strains to 5 mM H_2O_2 or to 50 nM mitomycin C during mid-logarithmic growth (Fig. 2A) or to 3 mM H_2O_2 and 50 nM mitomycin C during anaerobic stasis at day 14 in the rapid anaerobic dormancy (RAD) model (Fig. 2B). As the Δ*lsr2* strain could not grow well on solid agar, the liquid infinite dilution method was used to obtain an MPN measurement of viability. In contrast to previous data from *M. smegmatis*, the *M. tuberculosis* Δ*lsr2* strain displayed no statistically significant difference in survival in response to H_2O_2 from the wild-type strain during aerobic growth or in the RAD model (Fig. 2A and B). To ensure that the slowed rate of the Δ*lsr2* strain was not responsible for the lack of susceptibility to H_2O_2, we exposed all strains to either 3, 4, or 5 mM H_2O_2 under 2% oxygen, a condition during which all strains grew the same. We also exposed the cultures to 500 nM mitomycin C to determine if the Δ*lsr2* strain was more sensitive to DNA damage under hypoxic conditions. Under hypoxic conditions, the Δ*lsr2* strain was no more sensitive to all concentrations of H_2O_2 tested or to either concentration of mitomycin C (see Fig. S4 in the supplemental material). These data indicate that Lsr2 does not play a role in protection against DNA damage from oxidative stress and other
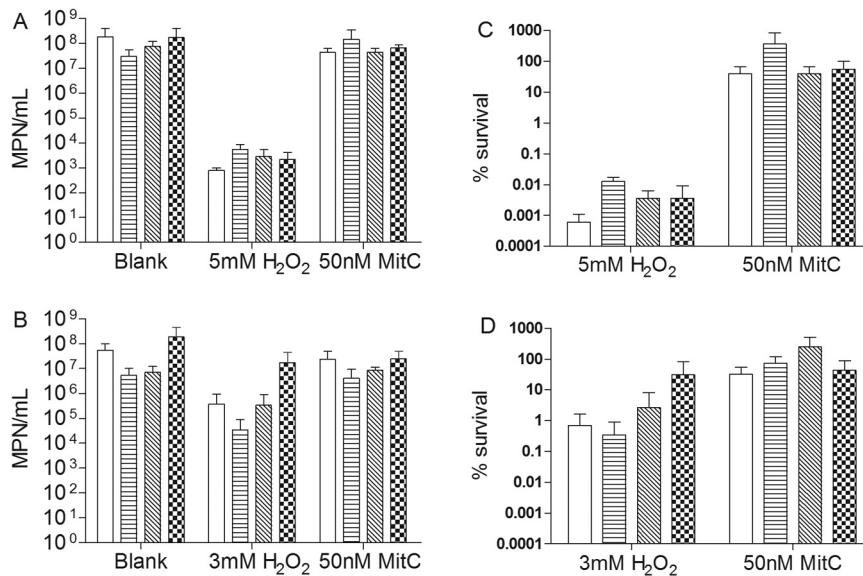
FIG 2 Survival of the Δ*lsr2* strain after addition of H_2O_2 or mitomycin C during aerobic growth or in an anaerobic model. Cultures of H37Rv (white bars), the Δ*lsr2* strain (horizontally striped bars), the Δ*lsr2* complemented strain (diagonally striped bars), or the *lsr2* overexpression strain (checkered bars) were exposed to water, 5 mM H_2O_2, or 50 nM mitomycin C (MitC) during aerobic growth (A), and the most probable number (MPN) was determined after 48 h. (B) Cultures were exposed to either water, 3 mM H_2O_2, or 50 nM mitomycin C at day 14 in a RAD model, and the MPN was determined after 5 days. Panels C and D are the calculated percentages of survival from panels A and B, respectively.

DNA-damaging agents as indicated in *M. smegmatis*. However, overexpression of *lsr2* did confer increased resistance to H_2O_2 stress compared to the other strains under anaerobic conditions (Fig. 2B), indicating that an increase in *lsr2* expression may have a slight protective effect when oxygen is lacking, but overexpression did not increase resistance to H_2O_2 under aerobic or hypoxic conditions.

Lsr2 is critical for adaptation to anaerobiosis. As the Δ*lsr2* strain had clear defects in adaptation to changes in oxygen levels, its ability to survive anaerobiosis was investigated. A modified RAD model was used to examine the adaptation and fitness of all strains to anaerobic conditions (11). The modified RAD model starts at a relatively high culture density with little available oxygen in order to prevent a high-oxygen growth phase that would be detrimental to the Δ*lsr2* strain. OD_{600} and MPN measurements were taken throughout the course of adaptation to and during maintenance of anaerobic conditions. As demonstrated in Fig. 3A and B, the OD_{600} of the wild-type and Δ*lsr2* complemented cultures increased in the first 24 h. After the bacilli consumed available oxygen and adapted to the anaerobic environment, the OD_{600} slowly decreased. In the Δ*lsr2* strain, however, the OD_{600} decreased immediately and remained significantly lower than those of all other strains throughout the hypoxic and anaerobic experiments. Interestingly, the *lsr2* overexpression strain initially increased in OD_{600} more than that of either the wild type or the Δ*lsr2* complemented strain and remained at a higher OD_{600} throughout anaerobic stasis. MPN measurements were taken to assess viability. Figure 3C demonstrates that there was no significant difference in survival rates among all four strains up to day 14 in the anaerobic model. By day 21, however, the Δ*lsr2* strain demonstrated a marked decrease in survival compared to all other strains. Although the *lsr2* overexpression strain displayed a higher OD_{600} throughout the experiment, this strain did not demonstrate a measurable increase in growth or survival.

Lsr2 is critical for recovery from anaerobiosis. To determine if Lsr2 is also important for recovery from long-term anaerobiosis, anaerobic tubes of each strain were opened and exposed to aerobic conditions. Recovery from anaerobiosis was monitored at days 7 and 14 of the RAD model, both time points at which the Δ*lsr2* strain did not demonstrate a significantly decreased viability (Fig. 3C). OD_{600} measurements were determined once every 24 h to assess growth. After 7 days in the RAD model, the recovery growth rates of all four strains were the same as during aerobic growth (Fig. 4A compared with Fig. 1B). The wild-type, Δ*lsr2* complemented, and *lsr2* overexpression strains were able to readily reactivate from anaerobiosis at day 14, albeit with a slight lag. The Δ*lsr2* strain, however, had a significant lag in reactivation by day 14 in the RAD model (Fig. 4B). The doubling time of the mutant recovering from 14 days in the RAD model was pronounced by a statistically significant lag compared to the wild type (Table 1).

Lsr2 modulates a shift away from aerobic respiration. To investigate further the defect in adaptation to anaerobic conditions, we added methylene blue to RAD model tubes to analyze the oxygen consumption of all strains while adapting to anaerobic conditions. Methylene blue decolorization correlates with oxygen depletion in the RAD model (11). OD_{600} measurements were obtained at regular intervals until all oxygen had been consumed, as measured by complete methylene blue decolorization. As is shown in Fig. 5, the Δ*lsr2* mutant consumed oxygen much more rapidly within the first 48 h than all other strains. The strain overexpressing *lsr2* consumed oxygen more slowly than all other strains. The rate of oxygen consumption directly correlated with the OD_{600} measurements of the strains during adaption to anaerobiosis.

Punctate DNA staining is unchanged in the Δ*lsr2* strain. During anaerobiosis, a small proportion of *M. tuberculosis* bacilli displayed a punctate 4′,6-diamidino-2-phenylindole (DAPI)
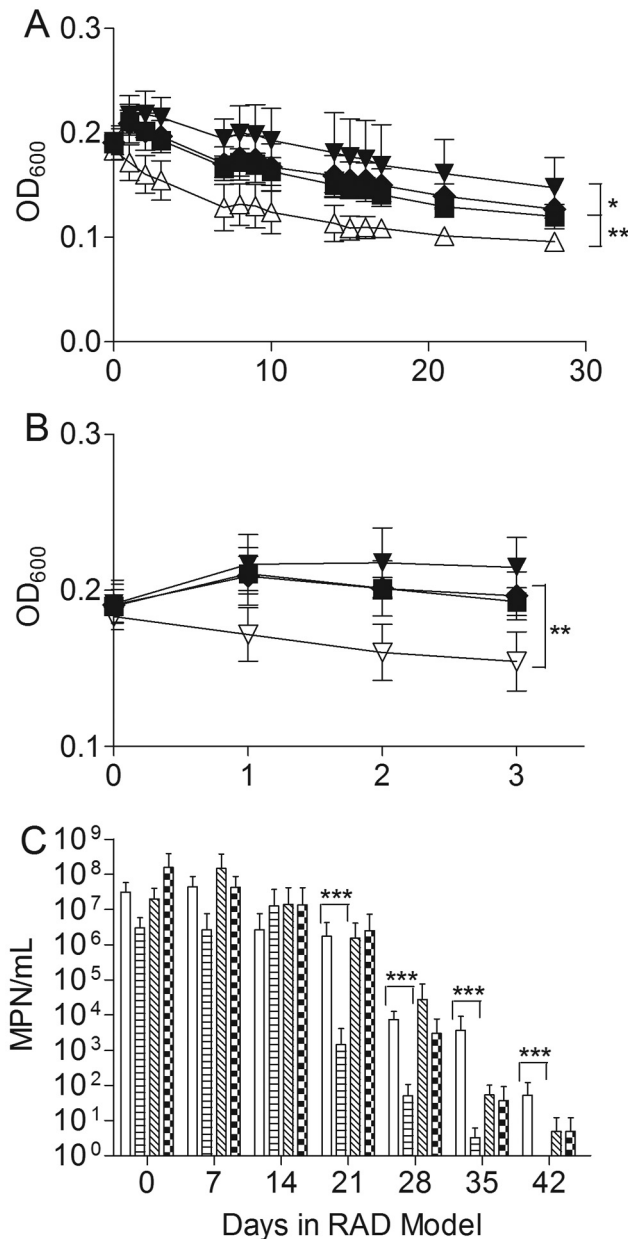
FIG 3 Growth and survival of the Δ*lsr2* strain in an anaerobic model. Cultures of H37Rv (squares and white bars), the Δ*lsr2* strain (open triangles and horizontally striped bars), the Δ*lsr2* complemented strain (diamonds and diagonally striped bars), or the *lsr2* overexpression strain (closed triangles and checkered bars) were cultured in the RAD anaerobic model. (A) OD$_{600}$ measurements were taken during the course of the RAD model. (B) OD$_{600}$ measurements during adaptation from aerobic to anaerobic phase of the model. (C) Viability MPN analysis at 0, 7, 14, 21, 28, 35, and 42 days in the RAD model.

staining pattern, which appears to indicate DNA condensation. If Lsr2 was involved in condensation of DNA during anaerobiosis, the difference in DNA nucleoid structure should be visualized using the DNA-specific stain DAPI. Both the wild type and the Δ*lsr2* strain were stained following anaerobic stasis and analyzed via microscopy. There were no visual differences between the wild type and the Δ*lsr2* strain in the compaction of DNA during anaerobiosis (see Fig. S5 in the supplemental material).

Lsr2 is a global transcriptional regulator. To determine the cause of heightened susceptibility of the Δ*lsr2* strain to an ambient oxygen environment or to an anaerobic environment, we performed whole-genome expression profiling by microarray analysis to compare wild-type gene expression to expression in the Δ*lsr2* strain during aerobic growth or after 24 or 48 h in a RAD model. A large set of genes was differentially regulated in the Δ*lsr2* strain (see Table S1 in the supplemental material). Most of these genes were also identified by chromatin immunoprecipitation with microarray technology (ChIP-chip) analysis of *M. tuberculosis* as being directly bound by Lsr2 (see Fig. S6 and Table S1 in the supplemental material) (5). The majority of genes directly controlled by Lsr2 from the ChIP-chip data were upregulated in the microarray experiments. These data indicate that Lsr2 is more prominent in gene repression than in gene activation. Many genes differentially regulated during aerobic growth were also differentially regulated in the RAD model. Some genes, however, were regulated by Lsr2 in the RAD model, which were not differentially regulated during aerobic growth (see Table S1). In order to understand why the Δ*lsr2* mutant was more susceptible to H$_2$O$_2$ in *M. smegmatis* but not in *M. tuberculosis*, we analyzed the transcriptional response of the *M. tuberculosis* Δ*lsr2* strain compared to that of the wild type after the addition of H$_2$O$_2$ during aerobic growth and at 48 h in the anaerobic model (see Table S1). Microarray analysis revealed that the genes responsible for responding to oxidative stress (e.g., *katG*, *trxC*, *trxB2*, *recA*, and *radA* [12]) were induced to similar levels in both the Δ*lsr2* and wild-type strains after H$_2$O$_2$ stress.

Lsr2 is critical for persistent infection. Lsr2 was important for survival during the changes in oxygen availability that are also experienced by bacilli during infection. Therefore, we tested H37Rv, the Δ*lsr2* strain, and the Δ*lsr2* complemented strain for *in vivo* growth and pathogenesis in BALB/c mice after aerosol infection (Fig. 6). Equal genome equivalents were detected for all three strains up to 2 weeks into infection. However, genome equivalents fell in the lungs of the mice with Δ*lsr2* strain infections by 4 weeks of infection (Fig. 6A). There were equal genome equivalents detected in the spleens of mice infected with all three strains at each time point (Fig. 6B). The numbers of genome equivalents detected for the wild type and the Δ*lsr2* complemented strain were comparable to CFU counts obtained by plating these 2 strains on 7H11 agar plates (Fig. 6C). Histopathology analysis was performed on lungs of infected BALB/c mice, and disease severity was scored. As shown in Fig. 6D, the Δ*lsr2* strain displayed no visible disease pathology in lung tissue at any time point, whereas the wild-type strain and the Δ*lsr2* complemented strain displayed significant disease by 4 weeks of infection. Histology analysis was performed on the lungs of 5 mice sacrificed at either 2 or 4 weeks post-aerosol infection (Fig. 7). Whereas inflammatory lesions were visible in mice infected with the wild type and the Δ*lsr2* complemented strain (Fig. 7A, B, E, and F), there were no signs of inflammation or any inflammatory lesions present within lungs of mice infected with the Δ*lsr2* strain (Fig. 7C and D).

Survival of the Δ*lsr2* strain after long-term exposure to nitric oxide. The oxidative burst within a mouse during *M. tuberculosis* infection occurs at around 2 weeks, and the nitrosative burst occurs at around 4 weeks (13). As the Δ*lsr2* strain did not display a defect until after 2 weeks of infection, we postulated the decrease in fitness of the mutant at 4 weeks could be due to sensitivity to RNS present during the nitrosative burst produced at later time
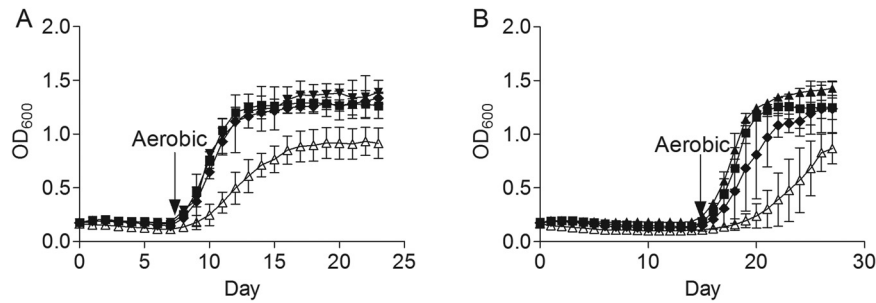
FIG 4 Recovery from anaerobiosis. H37Rv (squares), the Δ*lsr2* strain (open triangles), the Δ*lsr2* complemented strain (diamonds), or the *lsr2* overexpression strain (closed triangles) was added to RAD model tubes. After 7 days (A) or 14 days (B), tubes were opened as indicated by the arrows, all but 5 ml of culture was removed to ensure proper aeration, and the OD_{600} was obtained every 24 h.

points within the lung. We added six doses of 100 μM diethylene-triamine NONOate (DETA-NO), once every 6 h, to aerobic cultures and measured both recovery via OD_{600} and survival via MPN. The time to half-maximum value was calculated for each strain during recovery from long-term DETA-NO exposure and compared to that of the wild type. As demonstrated in Fig. S7A and S7B in the supplemental material, the Δ*lsr2* strain displayed delayed recovery after a prolonged exposure to nitric oxide compared with all other strains. None of these strains showed any decrease in viability after the addition of long-term DETA-NO exposure, as determined by MPN (data not shown) as we previously described for wild-type *M. tuberculosis* (12).

DISCUSSION

Lsr2 has been extensively studied in *M. smegmatis*, but Lsr2 in *M. tuberculosis* was believed to be essential (6, 10). We were successful in creating an *lsr2 M. tuberculosis* deletion mutant. We have demonstrated that the Lsr2 protein of *M. tuberculosis* is important both for survival in a high-oxygen environment and for adaptation to an anaerobic environment. The defect in growth at ambient oxygen levels likely explains the original designation of Lsr2 essentiality. The inability to grow under high oxygen tension could be due to increased susceptibility to ROS generated by the Fenton reaction during aerobic respiration (14), as an *M. smegmatis lsr2* deletion strain was more sensitive to H_2O_2 stress (9). However, the *M. tuberculosis* Δ*lsr2* strain was not more sensitive to exogenous H_2O_2, either aerobically or anaerobically. The aerobic growth defect in the Δ*lsr2* strain is not primarily due to a defect in H_2O_2 defense, but perhaps the *lsr2* mutant is defective in defense against other ROS. However, the genes most highly expressed after addition of H_2O_2 are not induced in the *lsr2* mutant, and the types of genes controlled by Lsr2 indicate that the lack of Lsr2 results in deregulation genes important for aerobic growth.

Lsr2 from *M. smegmatis* has also been implicated in the direct

protection of DNA. A study by Colangeli et al. demonstrated recombinant Lsr2 binds directly to pUC19 plasmid DNA *in vitro* and protects it against DNA-damaging agents. The authors speculated that Lsr2 could play a role similar to Dps in *E. coli*, condensing DNA during the stationary phase and protecting it against insults such as ROS (9). However, *M. tuberculosis* Lsr2 *in vivo* does not appear to have a direct role in protecting DNA from damage via condensation. This conclusion is based on several lines of evidence. First, the *M. tuberculosis* Δ*lsr2* strain is not more susceptible to DNA-damaging agents such as H_2O_2 or mitomycin C. Second, Lsr2 from *M. tuberculosis* binds and regulates a large number of genes throughout the genome in an AT-rich, sequence-independent manner, similar to the H-NS protein from *E. coli* (see Table S1 in the supplemental material and references 5 and 15). Third, DAPI staining of anaerobic *M. tuberculosis* (see Fig. S5 in the supplemental material) shows similar staining patterns, indicating that Lsr2 is not solely responsible for global DNA compaction, although it is likely that Lsr2 binding results in localized changes in tertiary structure. In addition, overexpression of Lsr2 in *M. tuberculosis* was not associated with global gene repression, indicating that it is not condensing DNA nonspecifically (6). The disparity between the results of Colangeli et al. and those of this study could be due to the fact that φX174 DNA was used to assess the role of Lsr2 as a protector of DNA *in vitro*. φX174 DNA has a high AT content (55%) (16) compared to *M. tuberculosis* (45%) (17), and Lsr2 readily binds to high-AT-content DNA. Thus, *in vitro* conditions and AT-rich DNA may have promoted nonspecific Lsr2 binding.

Whole-genome expression profiling demonstrated many genes were upregulated in the Δ*lsr2* strain, including several PE or PPE family proteins and genes that were horizontally acquired, such as *Rv2339*. These genes contain a higher AT content, to which Lsr2 readily binds (5). However, while many genes were differentially regulated in the Δ*lsr2* strain, genes highly responsive to H_2O_2

TABLE 1 Doubling time between day 1 and day 3 during recovery from anaerobiosis

Condition	Doubling time for:			
	H37Rv (wild type)	Δ*lsr2* strain	Δ*lsr2* complemented strain	*lsr2* overexpression strain
Aerobic growth	21.1 ± 0.6	29.7 ± 3.4	21.2 ± 0.3	22.8 ± 0.4
RAD model				
Day 7	30.6 ± 2.3	61.2 ± 17.1	30.6 ± 1.9	32.3 ± 2.2
Day 14	41.8 ± 5.8	144.3 ± 6.4[a]	103.7 ± 101.1	41.3 ± 1.7

[a] Statistically significant difference between H37Rv and the Δ*lsr2* strain with a P value of <0.05.
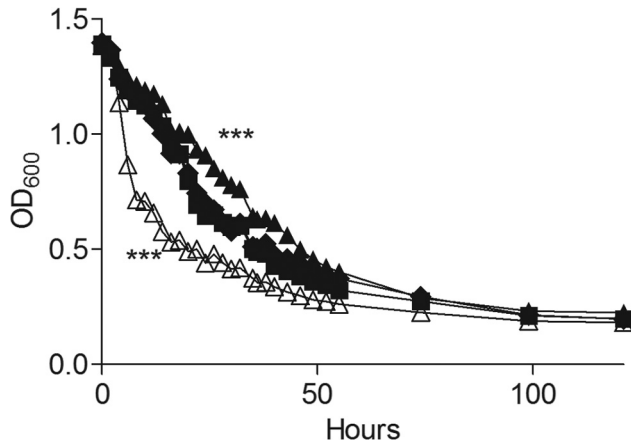
FIG 5 Oxygen consumption during adaptation to anaerobiosis as measured by methylene blue decolorization. H37Rv (squares), the Δ*lsr2* strain (open triangles), the Δ*lsr2* complemented strain (diamonds), and the *lsr2* overexpression strain (closed triangles) were added to a RAD model. Methylene blue (MB) was added (final concentration, 9 μg/ml) at time zero, and the OD_{600} measurement was taken at regular intervals until methylene blue decolorization was complete.

stress, such as *katG*, *trxC*, *trxB2*, *recA*, and *radA*, were not among them, further indicating that the defect in growth of the Δ*lsr2* strain is not due to sensitivity to ROS. Some genes that are normally upregulated by H_2O_2 stress were upregulated in the Δ*lsr2* strain in the absence of exogenous H_2O_2, such as the operon comprising *Rv1461* to *Rv1466* (*Rv1461-Rv1466*), involved in iron-sulfur cluster repair, *sigB* (an alternate stress sigma factor), *Rv2729*, and *Rv3018* (12). Some of these genes, such as *Rv1460* to *Rv1463*, are also upregulated under low-iron conditions (18). The

mmpL4 and *mmpS4* genes (*Rv0450* and *Rv0451*, respectively), were upregulated in the Δ*lsr2* strain and are normally repressed in the presence of high iron concentrations by the iron-responsive regulatory protein IdeR (18). The gene encoding the iron storage protein bacterioferritin (*bfrB*) was upregulated in the Δ*lsr2* strain and is directly bound by Lsr2. The upregulation of an iron storage protein could cause a decrease in available intracellular iron and consequently result in slower growth. The Δ*lsr2* strain is not likely more sensitive to the H_2O_2 produced during growth under aerobic conditions but may instead display slowed growth due to actual or perceived low-iron levels. Several genes (such as *Rv1067c*, *sigB*, *3288c*, *Rv3424c*, *Rv3879c*, and *Rv3903c*) that were expressed more highly in the Δ*lsr2* strain also respond to cell envelope disruption via addition of vancomycin (19). The *Rv1501-Rv1507c* operon involved in cell wall biosynthesis was upregulated in the Δ*lsr2* strain (20). The Δ*lsr2* mutant could be experiencing cell envelope stress due to differential regulation of genes responsible for cell wall biosynthesis. Cell envelope stress and low internal iron availability due to differential gene regulation in the mutant appear to be the main stresses that are being experienced by the Δ*lsr2* strain and could result in slowed to no growth under highly oxygenated conditions. Lsr2 is an important regulatory protein part of a larger regulatory network (21), the disruption of which clearly causes a severe growth defect during standard aerobic conditions.

Under constant hypoxia, the Δ*lsr2* strain had the same growth rate as the wild-type strain but displayed a growth defect during the microaerobic phase and a survival defect during the anaerobic phase in an anaerobic model. This discrepancy is likely because the oxygen concentration in the RAD model rapidly drops below the dissolved oxygen level in the 2% hypoxia experiment. Methylene blue starts to decolorize immediately in the RAD model but does not decolorize in the cultures under a 2% oxygen atmosphere. The
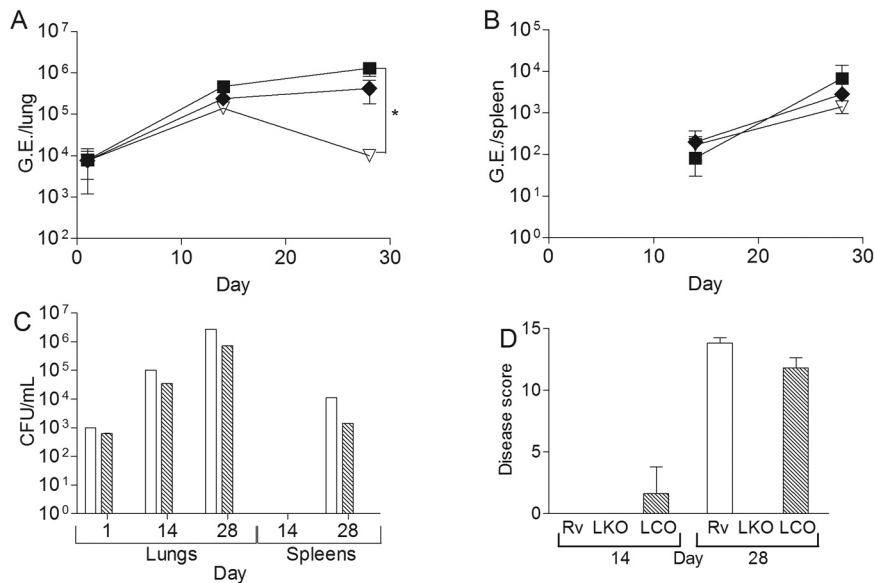

FIG 6 Survival of the Δ*lsr2* strain after aerosol infection in a BALB/c mouse model. Six- to 8-week-old BALB/c mice were infected via aerosol infection with either H37Rv (squares), the Δ*lsr2* strain (open triangles), or the Δ*lsr2* complemented strain (diamonds). Lungs (A) or spleens (B) were harvested at 1, 14, and 28 days, and genome equivalents (GE) were determined using qPCR with primer/probe sets for both Rv1738 and Rv2626. Genome equivalents were averaged together for both primer/probe sets. (C) CFU counts were obtained from lung and spleen samples for the wild type (white bars) and the Δ*lsr2* complemented strain (diagonally striped bars). (D) Disease scores were assessed for each mouse, and averages are shown for the wild type (Rv [white bars]), the Δ*lsr2* strain (LKO), or the Δ*lsr2* complemented strain (LCO [diagonally striped bars]). Five mice were used for each time point. An asterisk denotes differences that are statistically significant.
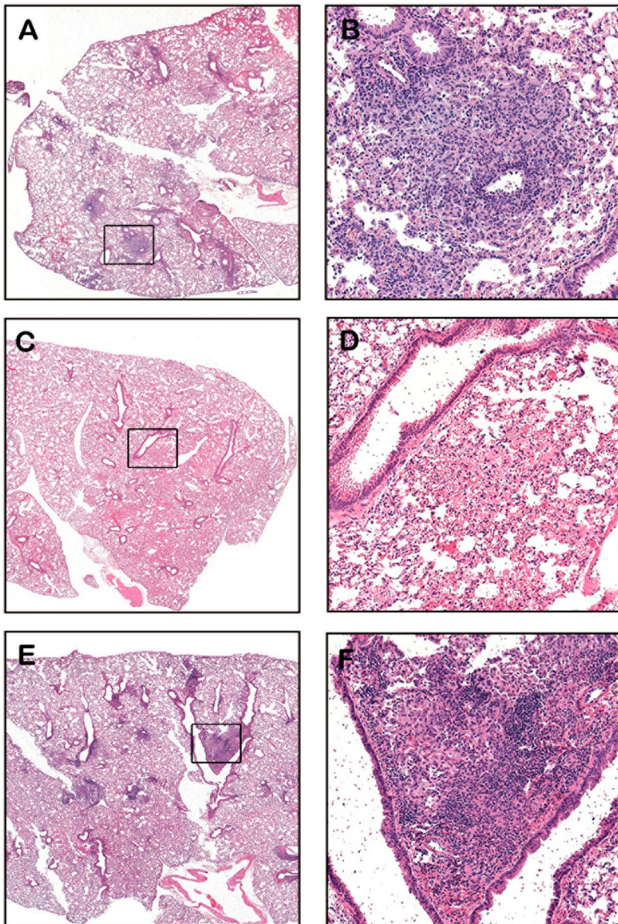
FIG 7 Histology of infected BALB/c mouse lungs using hematoxylin and eosin stain. BALB/c mice were infected by the low-dose aerosol method with the H37Rv strain of *M. tuberculosis* (A and B), the Δ*lsr2* strain (C and D), or the Δ*lsr2* complemented strain (E and F). Low-magnification photomicrographs (A, C, and E) or higher-magnification photomicrographs (B, D, and E) are shown.

ditions appears to be important for its survival. In addition, the rapid oxygen consumption of the Δ*lsr2* strain led to a shorter period of oxygen availability and less time for growth prior to the onset of anaerobiosis, during which obligate aerobes such as *M. tuberculosis* are unable to grow. The rapid oxygen consumption during microaerobic conditions is similar to that observed for a mutant with mutation of another key *M. tuberculosis* regulator, DosR, which is required for oxygen adaptation and anaerobic survival (11). A *dosR* mutant also consumes oxygen at a much higher rate than the wild type during microaerobic conditions and has a delayed recovery from anaerobic dormancy (11). A reciprocal trend was observed in the strain overexpressing *lsr2*, which had a slower oxygen consumption rate than the wild type and achieved a higher OD_{600} in the anaerobic model. As oxygen is required for *M. tuberculosis* growth, these data suggest that conservation of oxygen by the bacilli in this model allowed for more growth due to the longer time interval in the presence of oxygen (Fig. 5 compared with Fig. 3). As *M. tuberculosis* faces both microaerobic conditions and changing oxygen levels within the necrotic granuloma, Lsr2 should be important for survival within this environment.

The differential gene transcription profile displayed in this study correlated well with ChIP-chip data found by Gordon et al. (5), demonstrating that control of transcription by Lsr2 is mostly direct. A higher proportion of genes identified in the ChIP-chip analysis were also found by microarray analysis to be upregulated rather than downregulated in the Δ*lsr2* strain, indicating Lsr2 plays a greater role in gene repression than in gene activation. The Lsr2 protein in mycobacterial species has a similar function to that of the H-NS protein from *E. coli* (3–6, 21). Like Lsr2, H-NS is a small, basic protein (8) that functions mainly to repress gene transcription (7). Like H-NS, Lsr2 is able to activate as well as repress genes by nonspecific binding to AT-rich regions of DNA, but the role in activation of genes by H-NS is less extensive and not well understood (8). Not all genes differentially regulated in the Δ*lsr2* strain are directly controlled by Lsr2. Regulators such as *sigB* and *whiB3* were differentially regulated in the Δ*lsr2* strain, are either directly or indirectly controlled by Lsr2 (21), and are likely responsible for some of the indirect gene regulation in the mutant. The combination of direct binding studies and expression profiling demonstrates that Lsr2 directly regulates a multitude of genes important for growth at high and very low oxygen tension and survival during anaerobic stasis.

To determine if Lsr2 is required for pathogenesis, BALB/c mice were infected via aerosol infection with wild type, the Δ*lsr2* strain, and the Δ*lsr2* complemented strain from static growing cultures. The aerosol method of infection used in this study did not decrease the initial viability of the mutant, as genome equivalents detected on days 1 and 14 were similar for all three strains. After 4 weeks of infection, there was a significant decrease in genome equivalents detected in lungs of mice infected with the Δ*lsr2* strain. No notable disease pathology was observed in terms of lesion formation in mice infected with the Δ*lsr2* strain after 4 weeks, whereas in the mice infected with the complement and the wild-type strain, the pathology was clearly visible. These findings may be explained by the dynamics of the oxidative and nitrosative bursts within a murine *M. tuberculosis* infection. The oxidative burst within a mouse predominates within the first 2 weeks, whereas RNS exposure starts around 4 weeks into infection (13). The equal bacterial numbers in the lungs of all strains after 2 weeks

difference in growth rates for the Δ*lsr2* strain between early in the anaerobic model and the 2% oxygen atmosphere experiment indicates Lsr2 is required either for growth at the very low oxygen tension before anaerobiosis or for adaption to the rapidly declining oxygen tension that occurs in the aerobic to anaerobic model. The difference in growth rates as seen by OD_{600} was not reflected in survival as observed by MPN, but this is most likely due to the fact that this method of detecting viability is not as sensitive as plating for CFU, so small differences in viability will not be observed. Additionally, *M. tuberculosis* undergoes morphological changes during adaptation to anaerobiosis resulting in an increase in OD_{600} without a corresponding increase in CFU (22–24). Thus, the small decrease in OD_{600} observed in the Δ*lsr2* strain that is not reflected in the MPN of these cultures is likely due to changes in cell morphology of the mutant rather than to changes in viability. Lsr2 was also required for recovery after extended anaerobiosis. The anaerobic recovery and survival defects may be linked to uncontrolled rapid consumption of a dwindling oxygen supply during the shift to anaerobiosis. The ability of *M. tuberculosis* to slow the consumption of oxygen during adaptation to anaerobic con-

in the mouse were therefore not surprising, as the Δ*lsr2* strain was not more susceptible to H_2O_2 stress. Granulomas formed within a mouse do not become anaerobic (25); thus, the difference in viabilities at 4 weeks is likely not attributed to total lack of oxygen. We therefore speculate that this decrease in viability may be due to the presence of a nitrosative stress within the mouse lungs. Nitric oxide, like anaerobiosis, is a potent inhibitor of respiration (26). *M. tuberculosis* responds very similarly to nitric oxide and anaerobiosis and displays a similar pattern of growth arrest and slow recovery (11, 27). *In vitro* experiments demonstrated that the Δ*lsr2* strain displayed a prolonged lag in recovery when exposed to nitric oxide, similar to the delay in recovery observed from anaerobiosis. We speculate that a defect in recovery from a period in which aerobic respiration has been inhibited by a combination of limited oxygen and nitric oxide exposure may give the wild type an advantage over the Δ*lsr2* strain in the nonnecrotic BALB/c mouse model. The viability of the mutant was equal to that of the wild type at all time points in the spleen, indicating the splenic lesions were less restrictive with respect to respiration. As the bacterial counts were the same in the lungs for all strains at 2 weeks, the number of bacilli initially seeding the spleen would have been the same and likely accounts for the successful colonization of the spleen even though persistence in the lung was defective.

The life cycle of *M. tuberculosis* requires the pathogen to be transmitted via small aerosolized droplet nuclei that must penetrate deep into the lungs of a new host, where it is taken up within resident macrophages and neutrophils. These cells react to the growing bacteria by forming a hypoxic/anaerobic granuloma and applying antimicrobial agents, such as nitric oxide, that contain and control bacterial growth. Changes in oxygen availability during this infectious cycle are dramatic and numerous. During aerosol transmission, the pathogen is exposed to high oxygen tension in ambient air. The moment that the bacilli enter the lungs of a new host, oxygen levels rapidly drop, and they continue to decrease during granuloma formation. *In vitro*, Lsr2 is essential for growth on agar plates where the bacilli are exposed to air at an oxygen concentration of about 260 mg/liter, analogous to oxygen levels during aerosol transmission. Lsr2 is also essential for adaptation to microaerobic and anaerobic conditions, such as those found within necrotic lesions. Lsr2 is important for recovery from nonrespiring states after prolonged anaerobiosis or after exposure to nitric oxide, both of which are present during human infection. From the data presented herein, Lsr2 is a global transcriptional regulator similar to H-NS that directly controls gene expression in response to changes in oxygen availability. Lsr2 is important for persistent infection and likely plays a role in several stages of infection in which oxygen levels and the corresponding metabolic systems are in constant flux.

MATERIALS AND METHODS

Culture conditions, strains, and plasmids. Liquid cultures of *M. tuberculosis* strain H37Rv, the *lsr2*$^{\Delta174-268}$ strain (here referred to as the Δ*lsr2* strain) which was deleted for the C-terminal portion of the protein responsible for binding to DNA (5), the Δ*lsr2*::pMV306-*lsr2* strain (Δ*lsr2* complemented strain), and a strain of H37Rv containing the expression vector pMV261 (28) containing the gene for *lsr2* (here referred to as the *lsr2* overexpression strain) were maintained in Dubos-Tween-albumin broth (DTA) (Difco Dubos broth base [Becton Dickinson], 0.5% bovine serum albumin [BSA] fraction V, 0.75% glucose, 0.17% NaCl, and 0.05% Tween 80) as semisettled cultures at 37°C in flasks with daily agitation to ensure slight aeration. These low-aeration cultures were used to start all

experiments listed below, as all strains grew at the same rate under these hypoxic conditions as they did in defined 2% oxygen (Fig. 1A). The *lsr2* overexpression strain was maintained in the presence of 20 mg/ml kanamycin in order to maintain the pMV261 plasmid. Cultures were maintained at an OD_{600} of less than 0.5. All aerobic survival experiments after exposure to H_2O_2, mitomycin C, or diethylenetriamine NONOate (DETA-NO) were carried out at a starting OD_{600} of 0.1 in 10-ml volumes in glass tubes (20 mm by 125 mm) containing stir bars (12 mm by 4.5 mm). Growth of H37Rv, the Δ*lsr2* strain, the Δ*lsr2* complemented strain, and the *lsr2* overexpression strain in ambient air (~18% oxygen), 60%, and 2% oxygen concentrations was conducted in an oxygen-controlled chamber (Coy Laboratories). Ten-milliliter volumes of culture with a starting OD_{600} of 0.05 were maintained in 20 mm by 125-mm glass tubes containing 12- by 4.5-mm stir bars, and OD_{600} measurements were obtained daily. The modified rapid anaerobic dormancy (RAD) model was performed as follows (11). Sixteen-milliliter cultures at an OD_{600} of 0.15 were started in glass tubes (16 by 125 mm) containing stir bars (12 mm × 4.5 mm). Minimal headspace remained in the tubes (~1 ml). The tubes were sealed with caps containing butyl rubber septa and stirred at 60% of maximum speed using a rotary magnetic tumble stirrer from V & P Scientific (San Diego, CA). Methylene blue (final concentration, 9 μg/ml) was added to a set of tubes in order to assess oxygen depletion by all strains, and OD_{600} was obtained at regular intervals over a period of 4 days, or until the methylene blue became completely decolorized. Recovery from anaerobiosis was assessed by removing the lids from days 7 and 14 in the RAD model, with all but 5 ml of culture from the glass tubes removed to ensure proper aeration. Tubes were covered with loose-fitting caps, and the OD_{600} was measured every 24 h. Each experiment was performed using three biological replicates.

Construction of the Δ*lsr2* strain and Δ*lsr2* complemented strains. The Δ*lsr2* strain was constructed as previously described (29–31). Briefly, flanking regions comprising upstream and downstream regions of the *lsr2* gene were amplified using the following primers: upstream forward primer TTTTTTTTTCCATAGATTGGAGACCCGTCAGCACCGCAGT, upstream reverse primer TTTTTTTTTCCATCTTTTGGACGCCGCCACCCATTGCTTC, downstream forward primer TTTTTTTTTGCATAGATTGCGGCTCGTCGTAACGGGCACA, and downstream reverse primer TTTTTTTGCATAGATTGCCTGCATGACCCGCTCGATTT. Flanking sequences for upstream and downstream regions of *lsr2* were amplified by PCR and cloned into the pAES0004S plasmid containing a hygromycin resistance cassette, which was confirmed by sequence analysis. The vector was then ligated into the phAE159 phasmid, which was electroporated into *M. smegmatis*, and the resulting phage was amplified to obtain a high-titer stock. The high-titer phage was used to infect *M. tuberculosis*, which was plated onto DTA plates containing hygromycin. Plates were incubated for 3 months instead of the typical 1 to 2 months in sealed bags, which eventually led to the growth of a small number of *lsr2* mutant colonies. Colonies were picked, and PCR analysis was used to confirm the presence of the hygromycin-gene flanking region and absence of the wild-type gene. Sequence analysis was performed on these PCR products from the wild type, the Δ*lsr2* strain, and the phasmid construct in order to further confirm the absence of the wild-type *lsr2* gene in the Δ*lsr2* strain (see Fig. S1B in the supplemental material). The Δ*lsr2* complemented strain was constructed using the integrative vector pMV306. The *lsr2* gene was amplified along with 200 bases of upstream DNA to include the native promoter. The Δ*lsr2* strain was electroporated with the complementing plasmid, and colonies were picked, grown in the presence of antibiotic, and confirmed for presence of the vector using PCR analysis. For the *lsr2*-overexpressing strain, the *lsr2* gene was amplified and inserted downstream of the *hsp60* promoter within the exogenous pMV261 plasmid. The overexpression plasmid was introduced into H37Rv by electroporation, and the presence of the vector was confirmed by PCR.

Infinite dilution to determine viability. As the Δ*lsr2* strain was unable to grow on agar plates as well as the wild type, the viabilities of all strains were determined using the infinite dilution method to obtain the most

probable number (MPN) of viability, as described previously (11). Briefly, 50 μl of culture was added to 450 μl of DTA medium in 24-well plates, and 10-fold serial dilutions were performed up to a 10^{-10} dilution. Plates were sealed with parafilm wax and placed in plastic bags in a 37°C incubator for 8 to 10 weeks. Viability was determined using the highest dilution to show growth. All experiments were plated in duplicate, and three biological replicates were performed for each experiment.

H2O2 and mitomycin C challenge. Either 5 mM H_2O_2, 50 nM mitomycin C, or water was added to cultures of aerobically growing H37Rv, Δ*lsr2*, Δ*lsr2* complemented, and *lsr2* overexpression strains at a starting OD_{600} of 0.1. Viability was determined at both 0 and 48 h by the infinite dilution method to determine MPN. Alternatively, RAD model cultures of all strains were started, and 3 mM H_2O_2, 50 nM mitomycin C, or an equal volume of water was added after 14 days in the RAD model, after which samples were collected at days 0 and day 5 after addition of stress to determine viability as measured by MPN.

Microscopic analysis. Staining of dormant cultures of the H37Rv and Δ*lsr2* strains was performed as previously described (11). Briefly, cultures were resuspended in 0.025 M HEPES with 0.02% Tween 80 (pH 7.75). The DNA-specific stain 4′,6-diamidino-2-phenylindole (DAPI) was added at a final concentration of 300 nM for 20 min at 37°C. Samples were washed once in HEPES-Tween, resuspended in a small volume of phosphate-buffered saline (PBS), viewed on a Nikon Eclipse TE200-U inverted microscope, and analyzed using MetaVue software.

Microarray analysis. Oligonucleotide microarrays were printed at the University of Colorado Anschutz Medical Campus using oligonucleotides purchased from Operon and were processed and prehybridized as previously described (26). RNA isolation and cDNA preparation, labeling and hybridization were performed as previously described (32). Microarrays were scanned using a GenePix 4000b scanner (Axon Instruments). The intensities of the two dyes at each spot were quantified using GenePix Pro 6.0 (Molecular Devices). Microarray-determined ratios were calculated from three biological replicates. The ArrayStar program (DNASTAR) was used to determine statistically significant regulated genes (33). Genes included in Table S1 in the supplemental material exhibited at least a 2-fold induction or repression ratio under at least one condition and had a significance analysis of microarrays (SAM) corresponding false discovery *q* value of zero.

BALB/c mouse infections. Six- to 8-week-old BALB/c mice (Jackson Laboratories) were rested for 2 weeks before aerosol infection. The mice were then aerosol infected with around 4,000 bacilli (per mouse) of H37Rv, the Δ*lsr2* strain, or the Δ*lsr2* complemented strain by the Glas-Col inhalation exposure system as previously described (34). Lungs were harvested from three BALB/c mice that were sacrificed at 1 day postinfection, or lungs and spleens were harvested from five mice that were sacrificed at 2 and 4 weeks postinfection. Samples were homogenized and were assessed for bacterial load via determination of genome equivalents. The right caudal lung was collected and preserved in 4% paraformaldehyde for histological analysis.

DNA isolation. To determine genome equivalents in mouse tissues, tissue samples were homogenized and suspended into 4.5 ml of DTA broth. Cellular material from 1 ml of homogenate was pelleted by centrifugation for 10 min at 13,200 rpm. This pellet was resuspended with 1 ml Trizol reagent (Invitrogen). Cells were disrupted using 0.1-[Merops: inline graphic #1]mm-diameter zirconia/silica beads (BioSpec Products) with 6- to 30-s pulses in a bead beater and were placed on ice between bead-beating steps. Cellular debris was separated from the cell lysate by centrifugation for 1 min at 13,200 rpm, and lysates were transferred to a new tube. Three hundred microliters of chloroform was added to each sample, and tubes were mixed for 15 s and then were allowed to sit 2 min at room temperature with occasional mixing. Centrifugation was performed at 13,200 rpm for 10 min, and the aqueous phase of each sample was removed. Five hundred microliters of filtered back extraction buffer (4 M guanidine thiocyanate, 50 mM sodium citrate, 1 M Tris base) was added to the organic phase of each sample, and samples were incubated at

room temperature for 10 min. Separation of aqueous and organic phases was attained by centrifugation at 12,000 rpm for 30 min. The aqueous phase of each sample was then placed in a new tube, 10 μl of glycol blue (Life Technologies) and 400 μl of isopropanol were added to each sample, and samples were incubated at room temperature for 10 min. DNA was pelleted by centrifugation at 12,000 rpm for 15 min at 4° C, and the supernatant was removed. The DNA pellet was washed twice with 70% ethanol. The ethanol was removed, the pellet was briefly allowed to dry at room temperature, and the DNA pellets were resuspended in 20 μl of nuclease-free water.

Determination of genome equivalents. Five microliters of purified DNA from mouse tissue was used per quantitative PCR (qPCR). The primer sets for two *M. tuberculosis* genes, *Rv1738* and *Rv2626*, were used to determine genome equivalents (35). The primer and probe sets were as follows: *Rv2626c* forward, CCGCGACATTGTGATCAAAG, reverse, GC TCTGAGATGACCGGAACAC, and probe, CGAACGCAAGCATCCAG GAGATGC; and *Rv1738* forward, CACTGGACCGTCGACATAT CG, reverse, CGGTCGGCCGGATTG, and probe, CCAACGCAGCCGTGCCT TCG. Five microliters of DNA purified from mouse tissue, 0.6 μl water, 1.6 μl (each) forward and reverse primers, and 1.2 μl corresponding probe were mixed with 10 μl of master mix (Roche), and reaction mixtures were added to a 96-well plate (Roche). Quantitative PCR was performed on a LightCycler 480 (Roche). All samples were compared to a standard curve, generated using a 10-fold dilution series of *M. tuberculosis* genomic DNA. The equation of the plotted trendline from the standard curve was obtained and used to calculate the number of copies of genomic DNA present within each experimental sample. The values herein represent the average between the data obtained from the two primer/probe sets.

Histological analysis. The right caudal lobe was harvested from each mouse at 2 and 4 weeks into infection and fixed in 4% paraformaldehyde in phosphate-buffered saline (PBS). Tissue sections were embedded in paraffin and cut to 5 μm, mounted on glass slides, deparaffinized, and stained with hematoxylin and eosin. Slides were examined by a veterinary pathologist (R. J. Basaraba) blinded to the treatment groups. Microscopic changes, including an estimate of lung involvement, number of lesions, lesion type, the extent of lesion necrosis, and the relative distribution of lesions (alveolitis, peribronchiolitis, and perivasculitis), were scored for each animal and totaled. Once treatment groups were revealed, the mean scores were calculated, the section that scored closest to the different treatment groups was digitally scanned, and photomicrographs illustrating relevant features were generated (Fig. 7).

Nitric oxide challenge. Recovery and survival of all strains after long-term exposure to DETA-NO were assessed as previously described (11). Briefly, 10 ml of aerobically grown cultures at a starting OD_{600} of 0.1 was stirred as described above. A 100 nM concentration of DETA-NO was added to cultures six times, once every 6 h, and OD_{600} measurements were monitored. A sample of culture from each tube was also taken at 0 and 48 h to determine survival via MPN using the infinite dilution method. The time to half-maximum OD_{600} was determined as previously described (36). Briefly, half-maximum growth was defined as (maximum OD_{600} − starting OD_{600}) divided by 2. Linear interpolation using the two OD_{600} measurements flanking the half-maximum OD_{600} was used to calculate the time to half-maximum OD_{600} for each strain. The time to half-maximum OD_{600} value for each strain was divided by the value calculated for the H37Rv strain from the same treatment group to determine a percentage of the wild type for each strain.

Statistical analysis. A two-way analysis of variance (ANOVA) test was used to determine statistical significance for survival and growth data. A Student's *t* test was used to determine statistical significance for all mouse data and DETA-NO survival data. In all cases, values of <0.05 were considered statistically significant.

Microarray data accession numbers. Microarray data are available at the NCBI Gene Expression Omnibus website (http://www.ncbi.nlm.nih .gov/geo/) under accession number GSE57948.

SUPPLEMENTAL MATERIAL

Supplemental material for this article may be found at http://mbio.asm.org/lookup/suppl/doi:10.1128/mBio.01106-14/-/DCSupplemental.

Figure S1, TIF file, 1.8 MB.
Figure S2, TIF file, 0.7 MB.
Figure S3, TIF file, 1.7 MB.
Figure S4, TIF file, 0.6 MB.
Figure S5, TIF file, 1.9 MB.
Figure S6, TIF file, 0.9 MB.
Figure S7, TIF file, 1.5 MB.
Table S1, XLSX file, 0.1 MB.

ACKNOWLEDGMENTS

REFERENCES

1. Dye C, Scheele S, Dolin P, Pathania V, Raviglione MC. 1999. Consensus statement. Global burden of tuberculosis: estimated incidence, prevalence, and mortality by country. WHO Global Surveillance and Monitoring Project. JAMA 282:677–686.

2. Tsai MC, Chakravarty S, Zhu G, Xu J, Tanaka K, Koch C, Tufariello J, Flynn J, Chan J. 2006. Characterization of the tuberculous granuloma in murine and human lungs: cellular composition and relative tissue oxygen tension. Cell. Microbiol. 8:218–232. http://dx.doi.org/10.1111/j.1462-5822.2005.00612.x.

3. Chen JM, German GJ, Alexander DC, Ren H, Tan T, Liu J. 2006. Roles of Lsr2 in colony morphology and biofilm formation of Mycobacterium smegmatis. J. Bacteriol. 188:633–641. http://dx.doi.org/10.1128/JB.188.2.633-641.2006.

4. Gordon BR, Imperial R, Wang L, Navarre WW, Liu J. 2008. Lsr2 of Mycobacterium represents a novel class of H-NS-like proteins. J. Bacteriol. 190:7052–7059. http://dx.doi.org/10.1128/JB.00733-08.

5. Gordon BR, Li Y, Wang L, Sintsova A, van Bakel H, Tian S, Navarre WW, Xia B, Liu J. 2010. Lsr2 is a nucleoid-associated protein that targets AT-rich sequences and virulence genes in Mycobacterium tuberculosis. Proc. Natl. Acad. Sci. U. S. A. 107:5154–5159. http://dx.doi.org/10.1073/pnas.0913551107.

6. Colangeli R, Helb D, Vilchèze C, Hazbón MH, Lee CG, Safi H, Sayers B, Sardone I, Jones MB, Fleischmann RD, Peterson SN, Jacobs WR, Alland D. 2007. Transcriptional regulation of multi-drug tolerance and antibiotic-induced responses by the histone-like protein Lsr2 in M. tuberculosis. PLoS Pathog. 3:e87. http://dx.doi.org/10.1371/journal.ppat.0030087.

7. Dorman CJ. 2007. H-NS, the genome sentinel. Nat. Rev. Microbiol. 5:157–161. http://dx.doi.org/10.1038/nrmicro1598.

8. Dorman CJ. 2004. H-NS: a universal regulator for a dynamic genome. Nat. Rev. Microbiol. 2:391–400. http://dx.doi.org/10.1038/nrmicro883.

9. Colangeli R, Haq A, Arcus VL, Summers E, Magliozzo RS, McBride A, Mitra AK, Radjainia M, Khajo A, Jacobs WR, Salgame P, Alland D. 2009. The multifunctional histone-like protein Lsr2 protects mycobacteria against reactive oxygen intermediates. Proc. Natl. Acad. Sci. U. S. A. 106:4414–4418. http://dx.doi.org/10.1073/pnas.0810126106.

10. Sassetti CM, Boyd DH, Rubin EJ. 2003. Genes required for mycobacterial growth defined by high density mutagenesis. Mol. Microbiol. 48:77–84. http://dx.doi.org/10.1046/j.1365-2958.2003.03425.x.

11. Leistikow RL, Morton RA, Bartek IL, Frimpong I, Wagner K, Voskuil MI. 2010. The Mycobacterium tuberculosis DosR regulon assists in metabolic homeostasis and enables rapid recovery from nonrespiring dormancy. J. Bacteriol. 192:1662–1670. http://dx.doi.org/10.1128/JB.00926-09.

12. Voskuil MI, Bartek IL, Visconti K, Schoolnik GK. 2011. The response of Mycobacterium tuberculosis to reactive oxygen and nitrogen species. Front. Microbiol. 2:105. http://dx.doi.org/10.3389/fmicb.2011.00105.

13. Adams LB, Dinauer MC, Morgenstern DE, Krahenbuhl JL. 1997. Comparison of the roles of reactive oxygen and nitrogen intermediates in the host response to Mycobacterium tuberculosis using transgenic mice. Tuber. Lung Dis. 78:237–246. http://dx.doi.org/10.1016/S0962-8479(97)90004-6.

14. Imlay JA. 2003. Pathways of oxidative damage. Annu. Rev. Microbiol. 57:395–418. http://dx.doi.org/10.1146/annurev.micro.57.030502.090938.

15. Gordon BR, Li Y, Cote A, Weirauch MT, Ding P, Hughes TR, Navarre WW, Xia B, Liu J. 2011. Structural basis for recognition of AT-rich DNA by unrelated xenogeneic silencing proteins. Proc. Natl. Acad. Sci. U. S. A. 108:10690–10695. http://dx.doi.org/10.1073/pnas.1102544108.

16. Benzinger R, Hofschneider PH. 1963. Biological melting curves for the "replicative form" of Phi X 174 DNA. Z. Vererbungsl. 94:316–321.

17. Cole ST, Brosch R, Parkhill J, Garnier T, Churcher C, Harris D, Gordon SV, Eiglmeier K, Gas S, Barry CE, Tekaia F, Badcock K, Basham D, Brown D, Chillingworth T, Connor R, Davies R, Devlin K, Feltwell T, Gentles S, Hamlin N, Holroyd S, Hornsby T, Jagels K, Krogh A, McLean J, Moule S, Murphy L, Oliver K, Osborne J, Quail MA, Rajandream MA, Rogers J, Rutter S, Seeger K, Skelton J, Squares R, Squares S, Sulston JE, Taylor K, Whitehead S, Barrell BG. 1998. Deciphering the biology of Mycobacterium tuberculosis from the complete genome sequence. Nature 393:537–544. http://dx.doi.org/10.1038/31159.

18. Rodriguez GM, Voskuil MI, Gold B, Schoolnik GK, Smith I. 2002. ideR, An essential gene in mycobacterium tuberculosis: role of IdeR in iron-dependent gene expression, iron metabolism, and oxidative stress response. Infect. Immun. 70:3371–3381. http://dx.doi.org/10.1128/IAI.70.7.3371-3381.2002.

19. Provvedi R, Boldrin F, Falciani F, Palù G, Manganelli R. 2009. Global transcriptional response to vancomycin in Mycobacterium tuberculosis. Microbiology 155:1093–1102. http://dx.doi.org/10.1099/mic.0.024802-0.

20. Anthony P, Moran OH, Brennan PJ. 2009. Microbial glycobiology: structures, relevance and applications. Elsevier, Oxford, United Kingdom.

21. Galagan JE, Minch K, Peterson M, Lyubetskaya A, Azizi E, Sweet L, Gomes A, Rustad T, Dolganov G, Glotova I, Abeel T, Mahwinney C, Kennedy AD, Allard R, Brabant W, Krueger A, Jaini S, Honda B, Yu WH, Hickey MJ, Zucker J, Garay C, Weiner B, Sisk P, Stolte C, Winkler JK, Van de Peer Y, Iazzetti P, Camacho D, Dreyfuss J, Liu Y, Dorhoi A, Mollenkopf HJ, Drogaris P, Lamontagne J, Zhou Y, Piquenot J, Park ST, Raman S, Kaufmann SH, Mohney RP, Chelsky D, Moody DB, Sherman DR, Schoolnik GK. 2013. The Mycobacterium tuberculosis regulatory network and hypoxia. Nature 499:178–183. http://dx.doi.org/10.1038/nature12337.

22. Wayne LG, Sohaskey CD. 2001. Nonreplicating persistence of Mycobacterium tuberculosis. Annu. Rev. Microbiol. 55:139–163. http://dx.doi.org/10.1146/annurev.micro.55.1.139.

23. Wayne LG, Hayes LG. 1996. An in vitro model for sequential study of shiftdown of Mycobacterium tuberculosis through two stages of nonreplicating persistence. Infect. Immun. 64:2062–2069.

24. Cunningham AF, Spreadbury CL. 1998. Mycobacterial stationary phase induced by low oxygen tension: cell wall thickening and localization of the 16-kilodalton alpha-crystallin homolog. J. Bacteriol. 180:801–808.

25. Aly S, Wagner K, Keller C, Malm S, Malzan A, Brandau S, Bange FC, Ehlers S. 2006. Oxygen status of lung granulomas in Mycobacterium tuberculosis-infected mice. J. Pathol. 210:298–305. http://dx.doi.org/10.1002/path.2055.

26. Voskuil MI, Schnappinger D, Visconti KC, Harrell MI, Dolganov GM, Sherman DR, Schoolnik GK. 2003. Inhibition of respiration by nitric oxide induces a Mycobacterium tuberculosis dormancy program. J. Exp. Med. 198:705–713. http://dx.doi.org/10.1084/jem.20030205.

27. Park HD, Guinn KM, Harrell MI, Liao R, Voskuil MI, Tompa M, Schoolnik GK, Sherman DR. 2003. Rv3133c/dosR is a transcription factor that mediates the hypoxic response of Mycobacterium tuberculosis. Mol. Microbiol. 48:833–843. http://dx.doi.org/10.1046/j.1365-2958.2003.03474.x.

28. Stover CK, de la Cruz VF, Fuerst TR, Burlein JE, Benson LA, Bennett LT, Bansal GP, Young JF, Lee MH, Hatfull GF, Snapper SB, Barletta RG, Jacobs RJ, Jr, Bloom BR. 1991. New use of BCG for recombinant vaccines. Nature 351:456–460. http://dx.doi.org/10.1038/351456a0.

29. Bardarov S, Bardarov S, Jr, Pavelka MS, Jr, Sambandamurthy V, Larsen M, Tufariello J, Chan J, Hatfull G, Jacobs WR, Jr. 2002. Specialized transduction: an efficient method for generating marked and unmarked targeted gene disruptions in Mycobacterium tuberculosis, M. bovis BCG and M. smegmatis. Microbiology 148:3007–3017.

30. Bhatt A, Kremer L, Dai AZ, Sacchettini JC, Jacobs WR. 2005. Conditional depletion of KasA, a key enzyme of mycolic acid biosynthesis, leads to mycobacterial cell lysis. J. Bacteriol. 187:7596–7606. http://dx.doi.org/10.1128/JB.187.22.7596-7606.2005.

31. Brown AK, Bhatt A, Singh A, Saparia E, Evans AF, Besra GS. 2007. Identification of the dehydratase component of the mycobacterial mycolic

Lsr2 Is a Global Transcriptional Regulator

acid-synthesizing fatty acid synthase-II complex. Microbiology **153:** 4166–4173. http://dx.doi.org/10.1099/mic.0.2007/012419-0.

32. **Wilson M, Voskuil M, Schnappinger D, Schoolnik GK.** 2001. Functional genomics of mycobacterium tuberculosis using DNA microarrays. Methods Mol. Med. **54:**335–357. http://dx.doi.org/10.1385/1-59259-147 -7:335.

33. **Tusher VG, Tibshirani R, Chu G.** 2001. Significance analysis of microarrays applied to the ionizing radiation response. Proc. Natl. Acad. Sci. U. S. A. **98:**5116–5121. http://dx.doi.org/10.1073/pnas.091062498.

34. **Kelly BP, Furney SK, Jessen MT, Orme IM.** 1996. Low-dose aerosol infection model for testing drugs for efficacy against *Mycobacterium tuberculosis.* Antimicrob. Agents Chemother. **40:**2809–2812.

35. **Bartek IL, Rutherford R, Gruppo V, Morton RA, Morris RP, Klein MR, Visconti KC, Ryan GJ, Schoolnik GK, Lenaerts A, Voskuil MI.** 2009. The DosR regulon of *M. tuberculosis* and antibacterial tolerance. Tuberculosis (Edinb.) **89:**310–316. http://dx.doi.org/10.1016/j.tube.2009.06.001.

36. **Weiss A, Delproposto J, Giroux CN.** 2004. High-throughput phenotypic profiling of gene-environment interactions by quantitative growth curve analysis in *Saccharomyces cerevisiae.* Anal. Biochem. **327:**23–34. http://dx.doi.org/10.1016/j.ab.2003.12.020.